

## THE BAUXITE OF PORTO TROMBETAS

B. Boulangé & A. Carvalho

### Introduction

The Porto Trombetas deposits were discovered in 1950, and the open cut began in 1979. As all the Amazonian deposits, the profile shows five layers that are, from the top to the bottom: a kaolinitic layer, a nodular bauxite layer, a ferruginous nodular layer, a bauxitic layer overlying an another kaolinitic layer. These layers previously described in Porto Trombetas (Aleva, 1981; Grubb, 1979) were the object of a very recent detailed study with emphasis on the petrological characteristics and its geochemical and pedogenetic consequences (Lucas, 1989) (see chapter III).

The deposit of Porto Trombetas was also studied with more detail (Boulangé & Carvalho, 1989) but the objective was mainly concentrated on the geochemical aspect and particularly on the distribution of the Rare Earth Elements (REE).

### I. Regional aspects

The bauxite deposit of Porto Trombetas is located on the edge of the Rio Trombetas, and about 900 km east of Belém (Pará State). The lateritic bauxite deposits occur on various plateaux covering an area of more than 2,200 Km<sup>2</sup>. These high plateaux are deeply cut, with altitudes varying from 160 to 190 m (Fig. I.1). With a gentle dip (1 to 5°) toward the Amazon river, they present convex slopes that can attain 30°. They overlook a large morphological unit, with altitudes varying from 100 m at the foot of the plateaux to 70 m near the Amazon river that has its water level at 40 m.

The studied area was situated on the large plateau of Saracá. Despite being flat, its summit presents ondulations with altitudes varying from 175 m to 185 m. Locally small depressions, attaining more than 10 m of diameter and from 2 to 5 m deep, were also observed.

The region of Trombetas is situated in Low Amazon Basin, which is characterized by a clastic sedimentation of continental origin, laying in discordance over Paleozoic sediments. It is the Alter do Chão Formation, dated Upper Cretaceous or more precisely, Aptian-Turonian (Daemon, 1975). Its thickness exceeds 600 m and is constituted by clayey

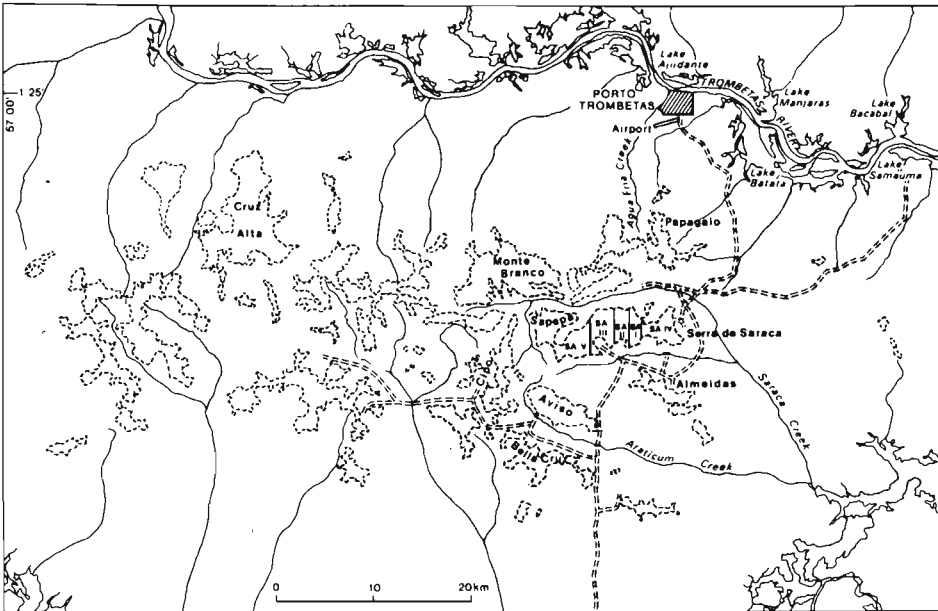


Figure I.1 - The bauxitic plateau of Porto Trombetas

sandstone, sometimes arcossian, intercalated with conglomerates, clay and siltstone.

The climate of this area can be considered as warm. The average temperature ranges from 24 to 26°C and the annual mean temperature normally exceeds 25°C. The temperature is high the whole year, particularly from September to November, when varies from 26 to 28°C. During June and July the temperature is milder but never below 22°C. On the other hand, it is a very humid climate, with 1,600 to 2,50 mm/year of rainfall. The precipitation is not evenly distributed throughout the year and the difference between the more humid and the dryer months is the largest of Brazil.

As concerning the vegetation the region of the so called firm land is covered by an hygrophile rain forest (Hiléia Amazônica). It is characterized by high trees with various strata. The other type is the evergreen forest that occurs in the valley bottoms. It presents smaller trees and lower number of species.

## II. Profile characteristic

The deposit of Porto Trombetas presents nearly the same gen-

eral characteristics of most of the other deposits of the Amazon Basin. The main difference refers to the thickness of the bauxitic layer, showing an average of 6 m and reaching 10 m in some regions.

The profile is rather homogeneous in the whole plateau (Fig. I.2) and presents practically the same sequence of horizons. They are the following, from the top to the bottom: upper kaolinitic layer; nodular bauxite layer; ferruginous nodular layer; bauxitic layer, lower kaolinitic layer and basal sediment.

### 1. Upper Kaolinitic layer

It is very homogeneous, yellow to reddish yellow downwards, without any apparent stratification. The thickness varies from 8 to 10 m on the plateaux and 0 to 5 m on the edges of the plateaux. It is constituted mainly of kaolinite (80%), gibbsite (10%) and quartz (10%). The kaolinite/gibbsite proportions have tendency to reverse toward the lower part, with a gradual transition to the nodular bauxite layer. The iron is present in a little amount as goethite in the upper part, and in a more important quantity as hematite in the nodular layer. In this kaolinitic ma-

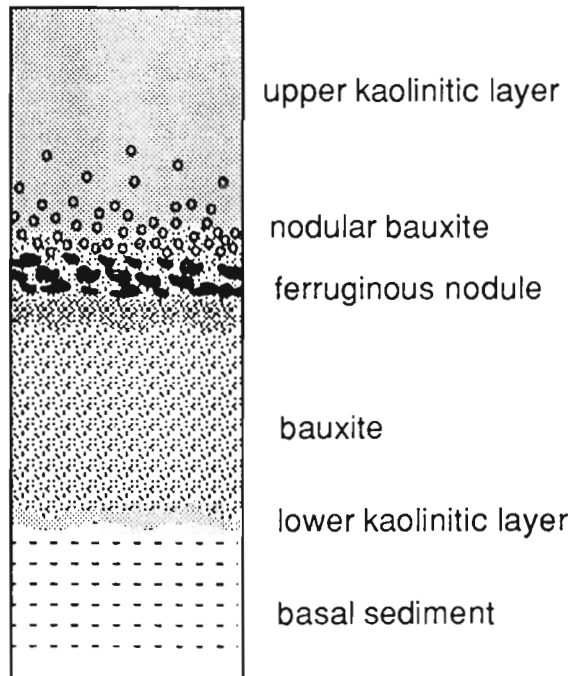


Figure I.2 - The bauxitic profile of Porto Trombetas

trix one can observe small quartz grains and small aluminous or ferruginous nodules in the following form:

- small quartz grains (less than 0.8 mm diameter) which show an angular and irregular shape. They present fissures and dissolution cavities penetrated by the clay matrix or sometimes filled up with a hematitic red product. This red product is totally enclosed within the limit of the quartz grains showing that it was formed before the matrix. Sometimes, mainly in the lower part of the layer, the quartz grains are coated with well-crystallized gibbsite;

- small round-shaped aluminous nodules (less than 0.5 mm diameter), constituted by gibbsite crystals that can reach the size of the nodule. They keep some local traces of the hematitic red product. The limits of the crystals are not clear and the gibbsite fades out in the matrix;

- small round-shaped ferruginous nodules (less than 0.5 mm diameter), red, argilomorphous, hematitic or goethitic.

The characteristics described above of both the quartz and the nodules seem to indicate that they were not transported. On the contrary, they would be originated by in situ transformation of a previous bauxite layer. The process would include deferruginisation with changing of hematite into goethite, and dissolution of the gibbsite. Part of the alumina undergoes resiliation to form kaolinite, and the rest is transferred to the subjacent bauxite.

## 2. Nodular bauxite layer (1 to 3 m)

These nodules are small (<5 cm) and with irregular shape. They are frequently coalescent forming sometimes true blocks, embedded in an yellowish red clay matrix. The nodules are heterogeneous, with a whitish violet nucleus. They are formed by porcellaneous gibbsite (very small crystals) showing at least three successive juxtaposed types, getting more and more clear towards the periphery. Each type is cut by a net of fractures fill up with well crystallized (sacharoid) gibbsite, that indicate their independence and thus, their succession through the time. In the lower part of these layer occur some ferruginous nodules that become gradually coarser. They form, by anastomosis larger fragments of irregular shape, vertically elongated, enveloping the ferruginous round spots that increase in diameter downwards. Finally, this layer changes into the underlying one through a transitional zone (10 cm);

## 3. Ferruginous nodular layer (1 m)

It presents, in the upper part (30 cm), nodules of about 10 cm,

cemented by a hard pinkish gibbsitic matrix. In the middle part (60 cm) they are embedded in a brownish yellow argilomorphous matrix. In the lower part, the ferruginous nodules are again cemented by a pinkish gibbsitic matrix forming a true crust. The nodules are reddish violet, hard and with irregular outline, without any coating. Under the microscope they present as very porous material formed by a red hematitic matrix. The pores are empty or sometimes filled in with well crystallized gibbsite. Some pores can present in its interior a small quartz relict. It seems that these nodules result from a ferruginisation of a very quartzous material. The quartz would be submitted to a strong dissolution followed by a gibbsite accumulation in the dissolution voids.

#### *4. Bauxitic layer (1 to 6 m)*

The upper part (1 m) is alumino-ferruginous, compact, massive. It is locally capped by a very ferruginous crust with alumina rich pale zones, and iron rich dark zones. The lower part (5 m) of this bauxitic layer, the main mined level, is formed by a porous and friable bauxite. This bauxitic layer is cut by large vertical pockets containing residual blocks and fragments of bauxite and a yellowish red clay material. The bauxite presents different degrees of ferruginisation with pale to dark red colors. Under the microscope these bauxites appears as formed only by well crystalized gibbsite (saccharoid). Locally and upwards the bauxite form hematitic walls, delimiting large voids (up to 200  $\mu\text{m}$ ). Downwards the gibbsite crystals form aggregates, with only a slight porosity.

The transition to the underlying layer is quite gradual.

#### *5. Low kaolinitic layer*

It is a yellow to brown colored horizon. It presents alumino-ferruginous relict nodules with gibbsite and hematite, embedded in the clay matrix. The hematitic red nodules fade out in the goethitic yellow spots. The bauxite relict nodules are constituted by large gibbsite crystals, sometimes in association with quartz. The quartz grains are fractured and show irregular outline, marked by dissolution features. The fractures are coated by well crystallized gibbsite, that is restrict to the grain limit. These quartz grains with gibbsite seems to be also residual in the clay matrix. The contact between the gibbsite and the kaolinite would indicate a dissolution and a resilication of the gibbsite rather than a desilication of the kaolinite.

## 6. Basal sediment

The deepest layer of these profiles were observed in an open ditch in the northeastern border of the Saracá plateau. It presents as a stratified quartzo-argillous sediment. The quartz, disposed in millimetric layers, presents dissolution features penetrated by the clay material.

## III. Chemical composition

The samples were grouped according to their facies, and the results of the chemical analysis, for the major and trace, elements are shown in Table I.1 and Figures I.3, I.4 and I.5. Some REE analysis were carried out and the results are presented in Table I.1. The curves normalized to NASC (Gromet et al., 1984) are shown in Figure I.6.

There are some points to be considered, before going in the discussion of the chemical composition. The first one refers to the possibility of existing lithological discontinuities in the basal sediment. This would be the source of the variations found in the different facies. The other point, concerns to the presence, in the basal sediment, of quartz layers which contains a rather high concentration of heavy minerals bearing Ti and Zr. The quartz layers were not included in the analysis of the basal samples and the result could be affected. Thus, in order to make possible the discussion that follows, some premisses were established. It was assumed that the sediment is rather homogeneous, which is quite possible but not certain. It was also assumed, that the influence of the quartz layer in the composition of the basal sediment, would be negligible, considering its relatively low abundance.

The upper kaolinite is very homogeneous as concerning its chemical composition. The  $\text{SiO}_2$  et  $\text{Al}_2\text{O}_3$  contents reflects its argillo-quartzous nature. The  $\text{Fe}_2\text{O}_3$  content is low (about 8%) and the contents of  $\text{TiO}_2$  (2.8%) and Zr (up to 1640 ppm) are rather high. The contents of  $\text{TiO}_2$ , Zr and HREE are three times greater as compared to the bauxite layer. This agrees with the microscopic observation which evidenced a resilication process. Indeed this transformation would go with a volume reduction and a correlative increasing of the residual minerals, as anatase and zircon.

The nodular bauxite is rich in alumina (61%) and present a low content of  $\text{Fe}_2\text{O}_3$  (2%). The content of trace elements and REE are just slightly higher than the bauxite. The matrix here has a kaolinitic composition and is rich in  $\text{TiO}_2$  and Zr, which agrees with their residual behavior during the resilication process evidenced in the upper kaolinitic layer.

Table I.1 - Chemical composition (major and trace elements of samples of different horizons of bauxitic profile from Porto Trombetas. REE analysis of some samples are also included.

	BTS1	BTS 2	BTS 3	BTS 4	BTS 5	BTS 7	BTS 8a	BTS 8b	BTS 8c	BTS 9a	BTS 9b	BTS 10a	BTS 10b	BTS 11	BTS 12	BTS 13a	BTS 13b	BTS 14	BTS 15	BTS 16	BTS 03b	BTS 03a	BTS 02b	BTS 02a	BTS 01	BTS 00
	KAOLINITIC LAYER					NODULAR BAUXITE			Fe. LAYER			BAUXITE					CLAY LAYER				BASAL SEDIMENT					
						matrix			Fe nod			upper zone		lower zone												
						Al nod			matrix			pale		dark												
									nodules																	
SiO2	38,90	37,10	36,50	36,10	34,50	26,50	25,90	4,30	18,80	22,80	6,90	2,10	0,63	0,95	2,80	3,30	8,50	29,40	31,20	25,30	38,27	15,78	48,54	40,73	47,08	47,24
Al2O3	34,80	36,30	36,95	37,10	37,90	43,40	43,30	61,20	19,10	29,00	26,30	60,20	47,40	55,30	61,00	61,60	53,70	40,80	35,60	44,70	35,17	56,62	33,98	28,77	33,49	30,39
Fe2O3	8,40	8,60	8,15	8,20	7,90	7,40	9,20	2,20	50,30	31,10	45,60	5,00	25,50	13,70	3,30	2,80	6,60	8,05	15,40	7,25	9,49	3,96	2,64	18,68	5,88	8,42
TiO2	2,70	2,80	2,75	2,80	2,80	2,40	2,10	1,10	0,77	2,20	1,00	0,71	0,88	0,96	1,10	0,68	2,70	4,05	2,00	1,65	2,08	0,86	0,98	0,52	0,65	0,51
H2O	14,97	14,83	15,16	15,24	16,46	19,95	19,01	30,57	10,54	14,45	19,77	31,32	25,51	28,51	31,30	31,03	27,90	17,29	15,57	20,48	14,05	23,52	12,77	11,40	12,60	12,27
V	148	152	153	178	148	148	186	97	545	625	640	137	270	173	98	89	152	169	270	163	133	61	40	208	64	97
Cr	140	156	154	174	142	188	186	114	320	220	220	76	152	100	48	50	116	173	122	84	87	51	43	110	36	32
Ga	58	68	63	76	68	66	70	58	60	76	74	52	64	54	48	58	76	73	60	51	84	29	22	29	21	32
K	180	160	135	110	96	83	50	50	58	64	50	50	50	50	50	50	50	50	50	50	50	50	50	50	50	50
Zr	1320	1480	1550	1640	1600	1440	1360	640	640	1240	780	440	420	520	440	310	940	1580	800	720	535	228	340	180	207	122
Nb		70			70			34			23			32	42		58		40		54	23	31	21	22	5
Y		28			26			12			13			9	11		15		10		10	3	5	3	5	5
La		12,6			10			3,7			7,45			2,14	2,4		2,46		3,53		5,5	16	42	38	53	82
Ce		20,3			17,4			5,91			10,1			3,93	4,12		4,56		4,96		4,7	17	44	40	50	165
Nd		6,97			5,5			1,9			3,01			0,95	1,02		1,18		1,19		8,2	2,3	6	4,44	5,3	6,6
Sm		1,37			1,05			0,35			0,56			0,22	0,28		0,37		0,38		1,3	0,6	1	1	0,1	1
Eu		0,37			0,31			0,15			0,18			0,11	0,14		0,16		0,13		0,2	0,1	0,1	0,2	0,1	0,1
Gd		2,08			1,76			0,81			0,81			0,53	0,76		0,89		0,69		0,9	0,4	0,5	0,5	0,4	0,4
Dy		3,14			2,96			1,26			1,22			0,92	1,15		1,6		1,02		1,3	0,5	0,8	0,5	0,4	0,5
Yb		3,7			3,66			1,39			1,39			1	1,4		2		1,14		1,7	0,9	1,2	1	1	1,4
Lu		0,61			0,59			0,24			0,24			0,18	0,24		0,33		0,2							
∑REE		51,14			43,23			15,71			24,96			9,98	11,51		13,55		13,24		115,6	37,8	95,6	85,64	110,3	257
∑LREE		41,61			34,26			12,01			21,3			7,35	7,96		8,73		10,19		111,7	36	93,1	83,64	108,5	254,7
∑HREE		9,53			8,97			3,7			3,66			2,63	3,55		4,82		3,05		3,9	1,8	2,5	2	1,8	2,3
La/Yb		3,40541			2,7322			2,6619			5,3597			2,14	1,7143		1,23		3,0965		32,353	17,778	35	38	53	58,571

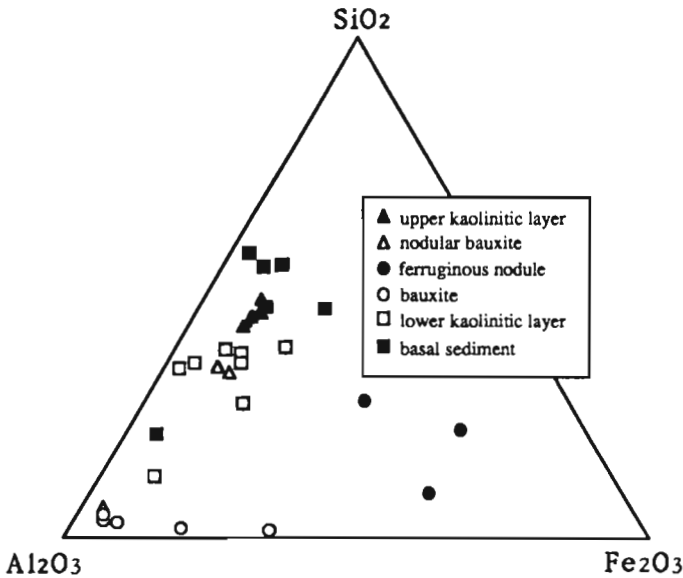


Figure I.3 - Samples of different horizons of bauxitic profiles of Porto Trombetas plotted in  $\text{SiO}_2$  -  $\text{Al}_2\text{O}_3$  -  $\text{Fe}_2\text{O}_3$  diagram.

The iron crust and the ferruginous nodules overlaying the bauxites are very rich in  $\text{Fe}_2\text{O}_3$  (45%) and show an excess of alumina, expressed as gibbsite in the dissolution voids. The matrix  $\text{SiO}_2/\text{Al}_2\text{O}_3$  ratio is similar to that of the kaolinite. The  $\text{TiO}_2$  content remains equivalent to the bauxite one (1%) but increases in the matrix (2%) (Fig. I.5). Zr and  $\text{TiO}_2$  present always a good positive correlation. V and Cr, as well as iron, show strong concentration. The HREE concentration is nearly the same as compared to the subjacent bauxite, but the La/Yb ratio presents a clear increase (5.3 times). The formation of this horizon occurs through an intense ferruginisation of the bauxite layer upper part. Thus, the absolute iron enrichment is followed by V, Cr and HREE concentration. The present evolution tendency is a deferruginisation that isolates relicts ferruginous nodules and gives origin to a kaolinitic matrix with strong concentration of residuals elements (Ti, Zr and HREE)

The bauxite has a very low grade in silica (<3%) and high content of  $\text{Al}_2\text{O}_3$  (50 to 60%). The  $\text{Fe}_2\text{O}_3$  content is low (<3%) but increases upwards, reaching 25% in the dark red zones. The  $\text{TiO}_2$  content is low, being only slightly higher than 1% (Fig. I.4). The V and Cr contents increase regularly with the iron content (Fig. I.5). In the bauxite layer, as compared to the basal sediment the Zr content is three times greater (Fig. I.4). On the other hand, the LREE content is lower while the HREE



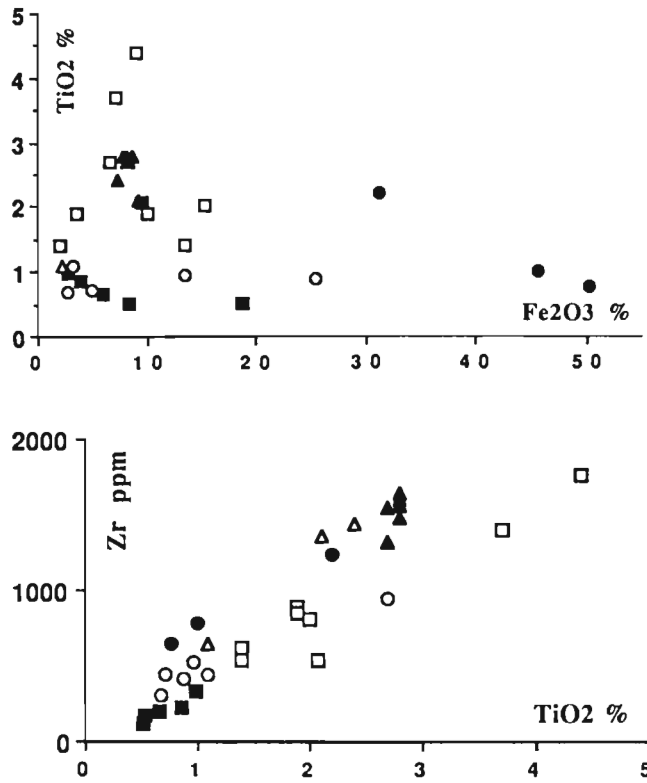


Figure 1.4 -  $\text{TiO}_2$  versus  $\text{Fe}_2\text{O}_3$  and Zr versus  $\text{TiO}_2$  of samples of different horizons of bauxitic profile from Porto Trombetas (For samples legend see Fig. 1.3).

content rest uniform, as indicates the decrease of the La/Yb ratio (1 to 2 in the bauxite and up to 60 in the sediment). Thus, the bauxite seems to present a composition that agrees with the basal sediment. The transformation (ferruginisation and desilication) would be performed with a volume reduction of 3 to 4 times, leading to a concentration of elements included in the residual minerals (anatase and zircons).

The lower kaolinitic layer present a lower silica/alumina ratio as considering the kaolinite composition. The excess of alumina corresponds to the presence of gibbsite. In addition, the content of  $\text{TiO}_2$  (2 to 4%) increases regularly upwards and it is higher as lower the iron content (Fig. 1.4). The limit with the subjacent bauxite is not clear and some samples (BTS 13b) mark the transition. The average Zr content increases towards the upper part of the horizon, where it is multiplied by a factor of 9 (1,580 ppm) as compared to the basal sediment (170 ppm). The REE contents decrease, but the HREE increase (La/Yb=3) with reference to

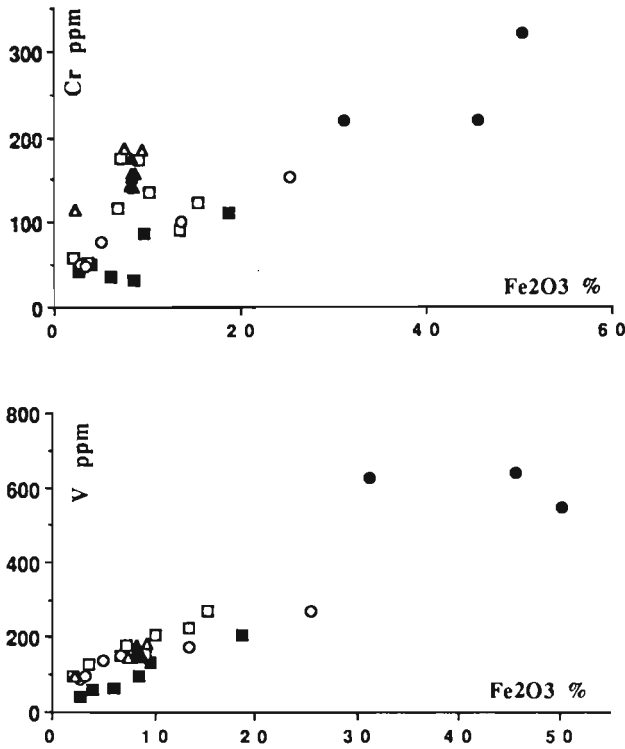


Figure I.5 - Cr versus Fe<sub>2</sub>O<sub>3</sub> and V versus Fe<sub>2</sub>O<sub>3</sub> of samples of different horizons of bauxitic profile from Porto Trombetas (For samples legend see Fig. I.3).

the basal sediment.

In the basal sediment only the kaolinitic material, not bearing quartz layers, was selected. The high SiO<sub>2</sub>/Al<sub>2</sub>O<sub>3</sub> ratio shows that this sediment is constituted essentially by quartz and kaolinite. These very white kaolinites are quite poor in Fe<sub>2</sub>O<sub>3</sub> (<3%), with red spots that contain up to 18% Fe<sub>2</sub>O<sub>3</sub>. The TiO<sub>2</sub> contents are very low (<1%) and increase towards the overlying layer. They are very homogeneous and in the diagram SiO<sub>2</sub>-Al<sub>2</sub>O<sub>3</sub>-Fe<sub>2</sub>O<sub>3</sub> (Fig. I.3), the samples are grouped together. Nevertheless, some samples (BTS 3a and 3b) presenting an intermediate composition, mark the transition between the basal clay sediment and the overlying kaolinites. The average trace elements contents are lower in the deeper horizon and increase toward the transition zone. The La/Yb ratio decreases strongly from the base to the transition zone (from 58 to 17), indicating a preferential leaching of the LREE.

The analysis of the ternary diagram SiO<sub>2</sub>-Al<sub>2</sub>O<sub>3</sub>-TiO<sub>2</sub> (Fig. I.4)

show that each facies has a definite chemical composition and the transitional terms are not well developed. The  $\text{TiO}_2/\text{Fe}_2\text{O}_3$  ratio (Fig. I.4) as a whole does not show a good correlation between these elements. Nevertheless, it seems that the  $\text{TiO}_2$ , in the form of anatase, behaves as a residual product. Thus, the lower kaolinitic layer and upper kaolinitic layer present the higher  $\text{TiO}_2$  content and the lower amount of  $\text{Fe}_2\text{O}_3$ .

Among the analyzed trace elements, the zirconium shows significant variations according to the facies (Table I.1). Thus, the medium values for the basal sediments (170 ppm) are multiplied by a factor of 2.3 in the bauxite (400 ppm), of 3.7 in the nodular bauxite (640 ppm) and up to 9 in the upper and lower clay. This important concentration of zirconium is associated with the presence of residual zircons, which are very resistant to the alteration. The  $\text{Zr}/\text{TiO}_2$  correlation (Fig. I.4) is rather good, which agrees with residual characteristic of these elements, preserved in the profile as anatase. It can be observed (Table I.1) that, Nb and Y show similar variation, marking as well the residual characteristics of these elements that could be included in the zircons (Gromet & Silver, 1983).

The vanadium and in less proportion, the chrome presents a good correlation with iron (Fig. I.5). It seems that they follow this element during the different phases of mobilization and transference. Thus, the ferruginous crust, resulting from an important absolute iron accumulation, presents the higher content of V (640 ppm) and Cr (up to 320 ppm).

The similarity of the REE spectra (Fig. I.6) seems to confirm that all the horizons, from the lower kaolinite up to the upper kaolinite layer, had similar origin. The presence of lower kaolinite layer, formed from the overlaying bauxite, reinforces the discontinuity between these bauxites and the basal sediment. Nevertheless the sample 3a seems to be an evidence of the affiliation between them. In addition, the variation of the HREE contents indicate a residual behavior, similar to the titanium and zirconium. On the contrary, the LREE are leached during the basal sediment bauxitisation and undergoes an absolute accumulation during the ferruginisation and resilication phases.

#### **IV. Genetic relationship of the horizons**

Despite the several studies carried out in the bauxites of the Amazon region, some aspects concerning their formation, are still a matter of discussion.

The objective of this paper, is to put out some aspects that could contribute to establish a model to these bauxites evolution. Neverthe-

less, it has be pointed out that, there is no idea of using the results obtained for Porto Trombeta deposit, to explain the origin of the Amazonian bauxite, as a general.

The kaolinitic upper layer, with no evident sedimentary structure, named Belterra Clay (Kotschoubey & Truckenbrodt, 1981), covers completely the bauxite layer. Its origin has been interpreted differently by various authors: as lacustrine deposits coming from the Andes region (Sombroeck 1966); as continental deposits following the bauxitization period, but related to the bauxites originated from the vicinity (Grubb, 1979; Kotschoubey & Truckenbrodt, 1981); as the upper part, extremely leached, of the continental deposits, named Barreiras Formation (Aleva, 1981; Dennen & Norton, 1977; Kistel, 1971); as an horizon resulting from pedogenetic evolution of a bauxite profile (Wolf & Silva, 1973; Lucas, in this book).

The petrological characteristics described previously, seem to indicate that they could not be transported. They would be originated by "in situ" transformation of a previous bauxitic and kaolinitic layer. The process would include deferruginisation with changing of hematite into goethite and dissolution of the gibbsite. Part of the alumina would suffer a resilication, forming kaolinite and the rest would be transferred to the subjacent bauxite. The process would involve a strong volume reduction, as suggested by the fact that the contents of  $TiO_2$  and Zr in this layer is twice or three times higher than in the subjacent bauxite. This could be used as well, to give an idea of the thickness of bauxite necessary to form the upper clay horizon. The enrichment in REE and the similarity of the spectra configuration, between the bauxite and the upper kaolinite, would confirm the residual character of this layer.

The main problem refers to the source of silica necessary for the upper kaolinite formation process, particularly considering that the present bauxite contains very few quartz. One possible explanation would be an external source for the silica. Nevertheless, the absence of sedimentary evidences and the geochemical continuity within the profile seems to contradict this hypothesis. Thus, it would be more reasonable to imagine an "in situ" origin.

In this case, the silica could be considered as originated only from the original sediment submitted to a strong volume reduction during its surficial evolution. The high concentration of Zircon could be an evidence of this volume reduction. As a matter of fact, the Zr constant calculation would evidenciate that 90 m of original sediment would be necessary to produce 1 m of upper kaolinite. Under this context, the  $SiO_2$  global losses would be very important, and a very low amount of

silica would go into the formation of the upper kaolinite.

The nodular bauxite is an horizon of alumina accumulation in the form of gibbsite. The gibbsite itself is now submitted to a degradation

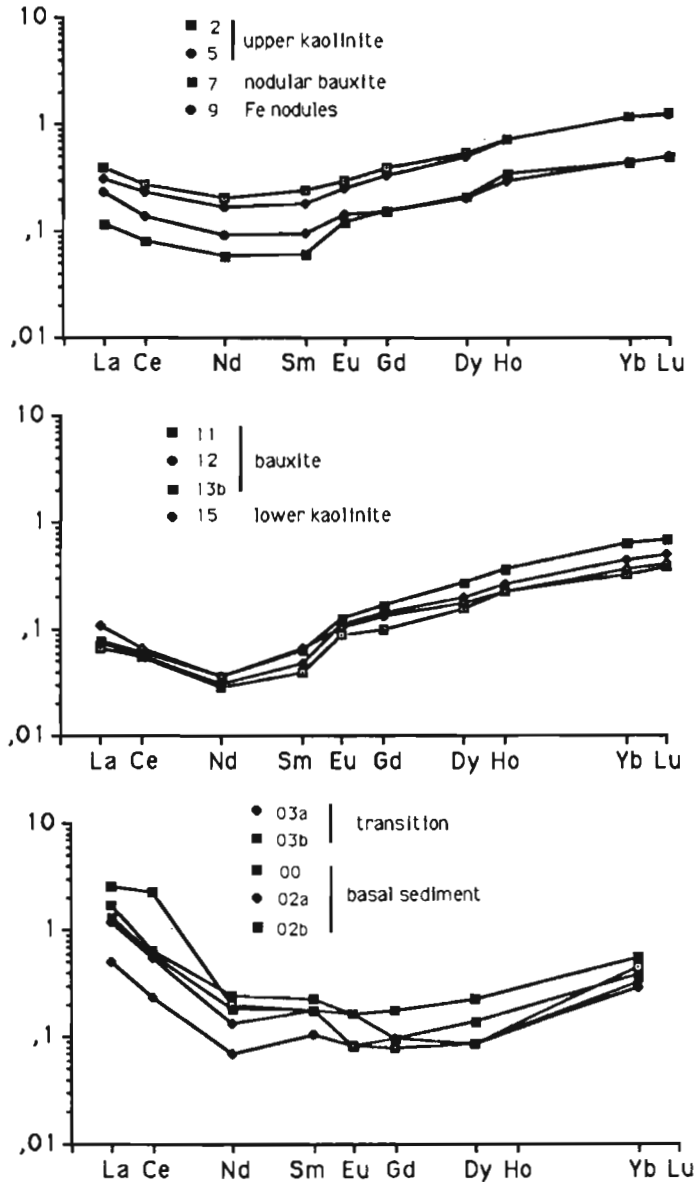


Figure I.6 - NASC normalized REE pattern for samples of different horizons of bauxitic profile from Porto Trombetas.

process. This is particularly evident in its upper part, where several generations of gibbsite nodules can be observed in the kaolinitic matrix. The low contents of  $\text{TiO}_2$  (1.1%), Zr (640 ppm) and REE in the aluminous nodules, would confirm the absolute accumulation of alumina. This alumina could be issued from the upper part existing bauxite degradation. The contents of  $\text{TiO}_2$  and Zr in the matrix are similar to those of the upper kaolinite, that underlines the present degradation process of these bauxite nodules.

The ferruginous nodules seem to be an iron accumulation horizon in a quartz layer. The same as the aluminium, the iron comes from an old subjacent profile. The vertical migration of both elements was separated in the time. The matrix characteristics show that these nodules, like the upper gibbsitic ones, are presently undergoing a degradation process (deferruginisation).

The bauxite results by the sediments transformation (Lucas cf. ch. III). The  $\text{TiO}_2$  and Zr contents are only slightly higher as compared to those of the basal sediment. This seems to confirm the idea that the bauxite formation from this sediment occurs with a rather low volume decrease and thus, preserving the original structure. Nevertheless, the sedimentary structures are no more evident and the volume preservation is only observed at a microscopic scale: ferruginous walls, delimiting cells invaded by the gibbsite. The REE content seems to indicate that, during this transformation the LREE are strongly leached. Meanwhile, the HREE, associated with the residual minerals (zircon), present a rather constant values. As it was mentioned before, it is also possible that this anomaly is due to the sampling bias.

The lower kaolinite layer seems to be a result of a bauxite recent transformation, submitted to a deferruginisation and resilication process. The  $\text{TiO}_2$ , Zr and HREE contents increase, show that these transformations occur together with a volume reduction, at the same proportion that in the upper kaolinitic layer.

It seems quite evident that the present tendency, in the profile as a whole, is not the bauxite formation but the deferruginisation and resilication.

## **V. Profile evolution**

The recent evolution shows that the horizons assembly is not a result of a sedimentary process, but of a long geochemical history. The thick sedimentary cover, under equatorial or humid tropical climatic conditions; was submitted to several transformation fronts, that has pro-

gressed downwards.

1. A weathering front, where the sediments were transformed according to the described process (Lucas et al., 1989). The process includes kaolinization followed by desilication and formation of gibbsite, giving origin to the bauxite;

2. A pedoturbation front, occurring on the upper part of the forming bauxite, where the skeleton and matrix are dissociated. The presence of this front is accompanied by a temporary hydromorphy that mobilizes the iron from the bauxite, with the alumina undergoing a residual accumulation as cryptocrystalline gibbsite.

3. A ferruginisation front where the iron previously mobilized is fixed;

4. A resilication front of the cryptocrystalline gibbsite, with the residual silica, always present in small amounts, in the bauxite as residual quartz or traces of kaolinite. This silica would be mobilized and brought back to the profile by the influence of the vegetation cover (Lucas et al., 1993);

The proposed schema for the profile evolution, based on the petrographic and chemical analysis and field observation is shown in Figure 1.7.

A. A weathering front (1) is installed on the sedimentary cover and through silica leaching and iron and alumina accumulation originates the bauxite. The iron content is low, since the sediment was poor in this element. The upper part of the bauxite, under the influence of the vegetation, is then submitted to a pedoturbation front (2), leading to the gibbsite partial deferruginisation and resilication. The resulting continuity between the bauxite and the upper kaolinitic layer is a consequence of the initial low iron content.

B. The weathering front (1) progresses into the original sediment, thickening the bauxite layer. At the same time, but at a smaller rate, the pedoturbation front (2) goes downwards in the bauxite. The upper residual bauxite horizon is affected by the resilication front (4) keeping its thickness rather constant. The mobilized iron is accumulated within the bauxite, subjacent to the ferruginisation front (3). This zone corresponds to the water table oscillation level. Thus, the iron content increases gradually in the bauxite.

C. All the four fronts deep down simultaneously. Bauxite and upper kaolinite layer get thicker. The amount of iron in the bauxite is more and more important.

D. The iron mobilized in the pedoturbation front, is fixed preferentially in a certain profile level, forming a real crust. This level is prob-

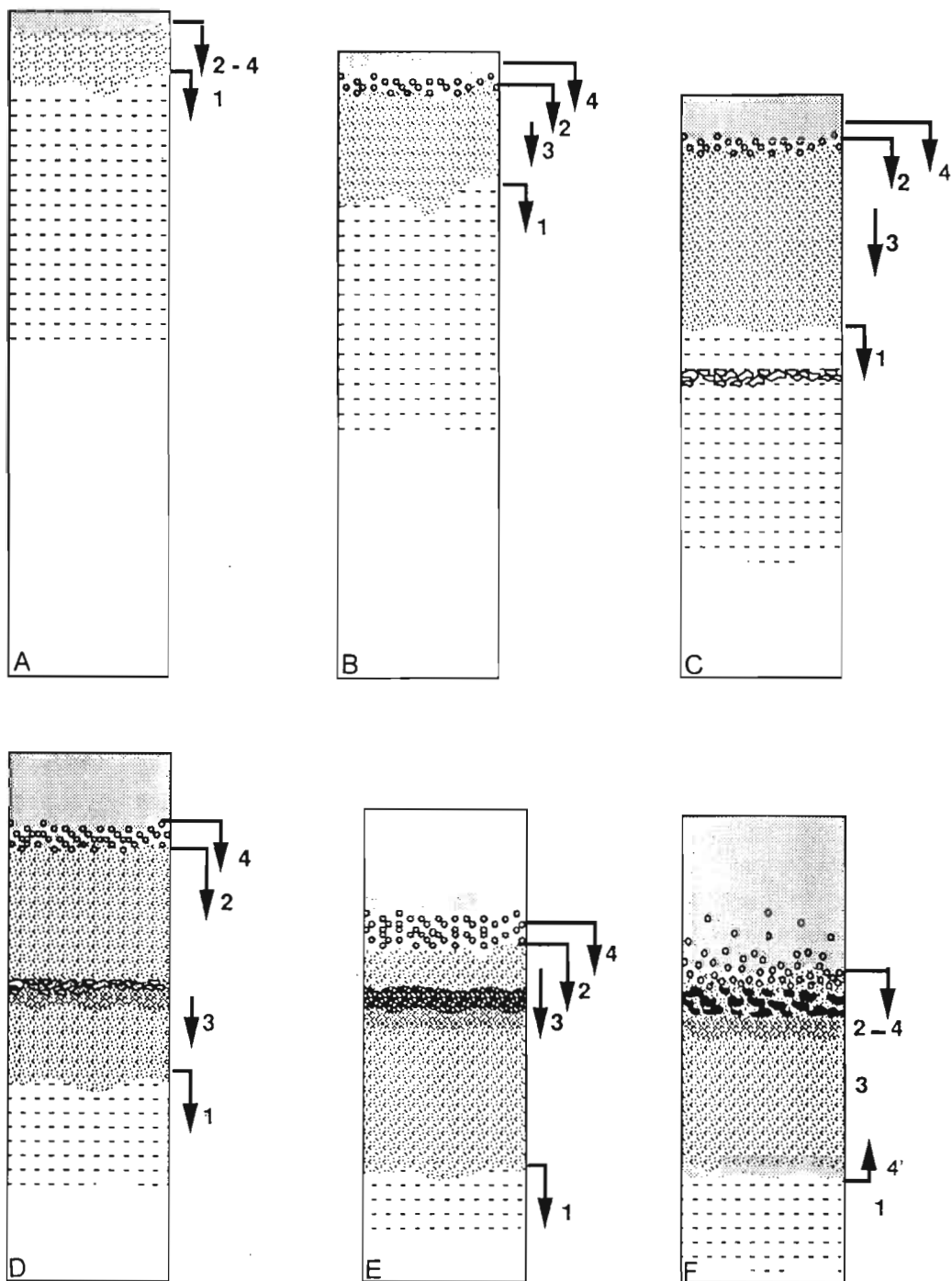


Figura I.7 - Stages of evolution bauxitic profile from Porto Trombetas.



ably associated to the original sediment structure (quartz layer). This iron immobilization, forming hematitic walls between the quartz grains, is susceptible to accentuate the quartz dissolution (Morris & Fletcher, 1987). This way, numerous voids are developed. Some of them are filled up with gibbsite coming from part of the alumina liberated in the pedoturbation front.

E. This iron crust development stops the pedoturbation front progression. The whole upper bauxite will be deferruginized, re-structured. The resilication front keep progressing, at the expenses of this bauxite.

F. This model originates the present profile, where the pedoturbation front is blocked by the iron crust. The resilication will keep on going, at the expenses firstly of the upper cryptocrystalline bauxite and later on, of the iron crust itself. This result in the present nodular facies. In the lower part of the profile, probably due to morphoclimatic conditions changes, the alteration front progression is also stopped. It is then developed, at the expenses of the bauxite, a lower resilication front (4').

It is rather difficult to know the morphological and climatic conditions that have existed on these plateaux, during the transformation of 90 m of sediment. In any case, it is hard to admit that the plateaux surface has been always flat. On the contrary, it is more acceptable that they were undulated. The plateau general morphology could be identified as a doline system, which would give origin to the topography undulations, which have varied through the time. Residual Al, Fe and Si have been continuously mobilized, due to the local hydromorphic conditions variations. The Fe would be trapped in a permeable quartzous sedimentary layer, forming a deep crust which has an effect on the present horizontal structure.

## **Conclusion**

The bauxite deposit of Porto Trombetas results from an in situ evolution of a thick layer of sediment. This evolution, that depends on biological and morphological factors, would occurred within a long period. Actually, up to now there is no defined hypothesis on the variation of the paleoclimatic and paleotopographic conditions during the bauxitization period. Nevertheless, known data on paleoclimatology (Parrish et al., 1982), show that during the late Cretaceous and the Tertiary, the Amazon Basin was submitted permanently to a very humid climate.

In a model of continuous evolution, the present profile would result from combining processes, including the formation of a ferruginous

bauxite and deferruginisation and resilication of this bauxite. The removed iron is accumulated in a layer of quartzous sediment forming a ferruginous crust that stops the system deepening. The present bauxite layer would be formed below this crust.

## References

- ALEVA, G.J.J. (1981). Essential difference between the bauxite deposits along the southern and northern edges of the Guiana Shield, South America. *Economic Geology and the Bulletin of the Society of Economic Geologists*, **76**:1142-52.
- AMARAL, S.E. (1954). Nota sobre a Serie das Barreiras no vale do Rio Tapajós. *Boletim da Sociedade Brasileira de Geologia*, **3**(1):. 29-50.
- BAHIA, R.R.; ABREU, F.A.M. (1985). O rift do Amazonas - sistema aulacogênico na Plataforma Amazônica. SIMPÓSIO DE GEOLOGIA DA AMAZÔNIA, 2., Belém, 1985. Anais. Belém, SBG-Núcleo Norte. v.1, p:222-41.
- CAPUTO, M.V. (1984). Stratigraphy, tectonics, paleoclimatology, and paleogeography of Northern Basins of Brazil. Santa Barbara, 586p. (Ph.D.Thesis - University of California).
- CAPUTO, M.V. (1985). Origem do alinhamento estrutural do Juruá - Bacia do Solimões. SIMPÓSIO DE GEOLOGIA DA AMAZÔNIA, 2., Belém, 1985. Anais. Belém, SBG-Núcleo Norte. v.1, p.242-58.
- DAEMON, R.F. (1975). Contribuição à datação da formação Alter de Chão, Bacia do Amazonas. *Revista Brasileira de Geociências*, **5**:78-84.
- DENNEN, W.D.; NORTON, H.A. (1977). Geology and geochemistry of bauxitic deposits in the Lower Amazon Basin. *Economic Geology and the Bulletin of the Society of Economic Geologists*, **72**(1):.82-9.
- GRUBB, P.L.C. (1979). Genesis of bauxite deposits in the Lower Amazon Basin and Guianas Coastal Plain. *Economic Geology*, **74**(4):.735-750.
- KISTLEL; P. (1954). Historical resume of the Amazon Basin. Petrobras, Relatório Interno 126. 10.
- KLAMMER, G. 1971. Uber plio-pleistozane Terassen und ihre Sedimente im Unteren Amazonas Gebiet. *Zeitschrift fur Gemorphologie*, **15**(1):.273-286.
- KOTSCHUBEY, B.; TRUCKENBRODT, W. (1981). Evolução poligenética das bauxitas do distrito de Paragominas Açailândia (Estados do Pará e Maranhão). *Revista Brasileira de Geociências*, **11**:193-202.

- LUCAS, Y.; KOBILSEK, B.; CHAUVEL, A. (1989). Structure, genesis and present evolution of Amazonian bauxites developed on sediments. *Travaux ICSOBA*, **19**(22):81-94.
- MONTALVÃO, R.M.E., BEZERRA, P.E.L. (1985). Evolução geotectônica do craton amazônico (Amazônia legal). durante o Arqueano e Proterozóico. In: SIMPÓSIO DE GEOLOGIA DA AMAZÔNIA, 2., Belém, 1985. Anais. Belém, SBG-Núcleo Norte. v.1, p. 282-97.
- PARRISH, J.T.; ZIEGLER, A.M.; SCOTese, C.R. (1982). Rainfall patterns and the distribution of coals and evaporites in the Mesozoic and Cenozoic. *Palaeogeography, Palaeoclimatology, Palaeoecology*, **40**:67-101.
- Projeto RADAMBRASIL, 1973, Folha SA 21, SA 22, SA 23.
- SANTOS, J.F (1984). A parte setentrional do Craton Amazônica (Escudo das Guianas). e a Bacia Amazônica. In: SCHOBENHAUS FILHO C.; ALMEIDA CAMPOS, D.; DERZE, G.R.; ASMUS, H.E. (eds.) *Geologia do Brasil*. Brasília, MME/DNPM. 501p.
- SOMBROECK, W.C. (1966). Amazon soils: a reconnaissance of the soils of the Brazilian Amazon Region. Holanda, CAPD, 292p.
- WOLF, F.A.M., SILVA, J.M.R. 1973. *Provincia bauxitífera da Amazonia*. Belém, DNPM. 35 p